Multivariate-Spline and Scale-Specific Solution for Variational Analyses

TOSHIO M. CHIN

RSMAS/MPO, University of Miami, Miami, Florida, and Jet Propulsion Laboratory, California Institute of Technology, Pasadena, California

TAMAY M. ÖZGÖKMEN AND ARTHUR J. MARIANO

RSMAS/MPO, University of Miami, Miami, Florida

24 April 2003 and 24 July 2003

ABSTRACT

A recipe for a cubic B-spline-based solution for multivariate variational formulation of a data analysis and assimilation problem is provided. To represent a signal whose smallest wavelength is L, the spline scale must be at most $L/2$, or approximately the Nyquist wavelength. This spline scale defines the computational grid, which tends to be coarser than the typical grid required for finite-difference discretization and hence offers a significant advantage in computational efficiency. The geostrophy–thin-plate model is introduced and applied to a set of analysis problems to demonstrate the effectiveness of the solution technique.

1. Introduction

Oceanic and atmospheric data, including in situ, station-based, and satellite-based measurements, are rarely obtained at coincidental locations with model or analysis grid locations. In practice these data are often locally interpolated before they are ingested into an assimilation or analysis machinery, even though the assimilation and analysis procedures themselves are in essence interpolation schemes. The local interpolation (preinterpolation) is thus redundant, and to eliminate this redundancy there needs to be an algebraically consistent definition of the geophysical variables at subgrid locations as well as over the grid points. The variational spline is a convenient technique with which to achieve this. It provides not only a natural way to incorporate the irregularly sampled data but also a computationally more efficient alternative to the standard finite-difference representation of a variational formulation. While the use and technique of a single-variate spline are well documented (e.g., Prenter 1975; Inoue 1986), a multivariate formulation is often more applicable to many geophysical fluid problems, as the equations governing their behaviors (e.g., Navier–Stokes, equation of state) tend to be multivariate. Multivariate splines, however, have few expositions in the literature. This note describes a solution method based on the cubic B-spline, a commonly used interpolation function with continuous first and second derivatives.

An advantage of the spline-based formulation is that it allows the computational grids to be defined in terms of the physical scales of the features of interest, such as mesoscale vortices and jets. The numerical inversion required for variational solution can be performed on a resolution defined by these phenomenological scales, instead of the model grid scale, which, by numerical stability requirements (e.g., Courant–Friedrichs–Levy condition), is often several times finer than such physical features. The spline-based-solution technique can hence be significantly more efficient than more customary approaches based on finite-difference discretization over the model grid. This note presents a numerical procedure for a multivariate solution based on cubic B-spline (section 2 and Tables 1–3), followed by demonstrations of its advantages in analysis of mesoscale sea surface features (section 3).

2. Multivariate variational spline

Variational formulation represents state-of-the-art data assimilation and analysis technology (e.g., Ghil and Malanotte-Rizzoli 1991). A generic variational formulation minimizes the discrepancy (''error'') between the solution and the data values, while maintaining a consistency toward some prior knowledge (''model'') expressed as a set of differential equations. The expressions for the model and data errors can be nonlinear in general. In practice, however, the nonlinear optimization problem is solved about a given initial solution (so-

Corresponding author address: Dr. Tamay Özgökmen, RSMAS/MPO, University of Miami, 4600 Rickenbacker Causeway, Miami, FL 33149-1098.
E-mail: tozgokmen@rsmas.miami.edu

called background fields) after a Taylor expansion, and the actual computation is an iterative solution of a sequence of linearized optimization problems. Such incremental and iterative corrections to the initial solution are made computationally feasible by local linearization of the model (i.e., construction of the so-called tangent linear model) and observation equations. For this reason, our presentation focuses on the spline solution for linear variational problems.

In this section, a general computational formula for multivariate variational spline is sought. Consider a generic I-dimensional spatial domain $\mathcal{D}$ whose coordinates, denoted as x_i, are bounded as $0 \le x_i \le X_i$ for $i = 1, \ldots, I$. Let the vector of the spatial coordinates be $\mathbf{x} \equiv (x_1, \ldots, x_I)$, so that

$$\mathbf{x} \in \mathcal{D} = [0, X_1] \times [0, X_2] \times \cdots \times [0, X_I].$$

Each unknown scalar field is denoted as $u_j(\mathbf{x})$ for $j = 1, \ldots, J$. For example, in the shallow-water model, u_1 and u_2 could, respectively, be the zonal and meridional components of the surface currents, while u_3 could denote the corresponding geopotential (pressure) field. Let $\mathbf{u}(\mathbf{x}) \equiv (u_1, \ldots, u_J)$ be the vector of the J unknown variables. In a linearized problem, $\mathbf{u}(\mathbf{x})$ can be the *perturbation* about a known background field.

a. The variational analysis problem

The prior model for the unknowns is given as a set of linear partial differential equations, which can be generically written as

$$\sum_{j=1}^{J} \sum_{\mathbf{n} \in \mathcal{N}} \mathbf{a}_{j\mathbf{n}} \nabla^{\mathbf{n}} u_j = \mathbf{b}, \tag{1}$$

where $\nabla^{\mathbf{n}}$ is a multidimensional differential operator defined as a product of derivatives, as

$$\nabla^{\mathbf{n}} \equiv \left(\frac{\partial}{\partial x_1}\right)^{n_1} \left(\frac{\partial}{\partial x_2}\right)^{n_2} \cdots \left(\frac{\partial}{\partial x_I}\right)^{n_I};$$

n_i is the order of the derivative along the ith spatial coordinate; $\mathbf{n} = (n_1, n_2, \ldots, n_I)$ is a vector of n_i, which is bounded as $0 \le n_i \le N_i$ for a given integer N_i for each i; $\mathcal{N}$ is the set of all possible values for the vector $\mathbf{n}$; and $\mathbf{a}_{j\mathbf{n}}$ and $\mathbf{b}$ are constant vectors. Note that $(\partial/\partial x_i)^0 \equiv 1$. The dimension of the (given) vectors $\mathbf{a}_{j\mathbf{n}}$ and $\mathbf{b}$ is equivalent to the number of partial differential equations used to model the unknown fields. The algebraic complexity of the model is determined by the number of nonzero $\mathbf{a}_{j\mathbf{n}}$. This is usually a small number (e.g., see section 3).

The (sparse) observations of the unknowns are denoted by their scalar values d_k and locations $\mathbf{x}_k^d$ for $k = 1, 2, \ldots, K$, where K is the number of the observations. The observation equation is assumed linear in u_j and written as

$$\sum_{j=1}^{J} c_{jk} u_j(\mathbf{x}_k^d) = d_k \tag{2}$$

for the given coefficients c_{jk}.

The optimal solution minimizes an objective functional that measures deviations from the model (1) and data (2). The standard, least squares formulation is adopted here. Specifically, the variational solution requires finding $\mathbf{u}$ that minimizes the least squares objective functional

$$\int_{\mathcal{D}} \left\| \mathbf{b} - \sum_{j=1}^{J} \sum_{\mathbf{n} \in \mathcal{N}} \mathbf{a}_{j\mathbf{n}} \nabla^{\mathbf{n}} u_j \right\|_{\mathbf{Q}^{-1}}^2 d\mathbf{x} + \sum_{k=1}^{K} \left[d_k - \sum_{j=1}^{J} c_{jk} u_j(\mathbf{x}_k^d) \right]^2 R_k^{-1}, \tag{3}$$

where $\|\mathbf{v}\|_{\mathbf{W}}^2 \equiv \mathbf{v}^{\mathrm{T}} \mathbf{W} \mathbf{v}$ denotes the squared norm of a column vector $\mathbf{v}$ weighted by a square matrix $\mathbf{W}$, the weighting matrix $\mathbf{Q}$ is the given model uncertainty covariance, and R_k is the given measurement error variance for the observed value d_k.

b. Spline representation of the geophysical fields

One way to compute the optimal solution of a variational problem is to first derive a set of partial differential equations (the Euler–Lagrange equations) from the objective functional. The differential equations must then be solved numerically for the solution $\mathbf{u}$. Alternatively, the continuous fields $\mathbf{u}$ can be parameterized first into a finite number of variables, which can then be evaluated directly as the solution of a discrete optimization problem. The latter approach is also known as the Rayleigh–Ritz method for finite-element approximation (Prenter 1975). We take this approach here.

Using the multidimensional spline basis functions $\phi_{\mathbf{m}}(\mathbf{x})$, the unknown field can be represented by a finite number of the gridded samples $u_{j\mathbf{m}}$ as

$$u_j(\mathbf{x}) = \sum_{\mathbf{m} \in \mathcal{M}} \phi_{\mathbf{m}}(\mathbf{x}) u_{j\mathbf{m}}, \tag{4}$$

where $\mathbf{m} \equiv (m_1, m_2, \ldots, m_I)$ and $\mathcal{M}$ are discrete versions of the spatial coordinates $\mathbf{x}$ and domain $\mathcal{D}$, respectively. Each spatial index m_i is an integer index, as illustrated below. The spline basis $\phi_{\mathbf{m}}(\mathbf{x})$ is a cross-product of the one-dimensional *generating function* $\phi(x)$, scaled along each spatial axis, as

$$\phi_{\mathbf{m}}(\mathbf{x}) \equiv \prod_{i=1}^{I} \phi_{m_i}(x_i) \equiv \prod_{i=1}^{I} \phi\left(\frac{x_i}{\Delta x_i} - m_i\right), \tag{5}$$

where Δx_i is the *scale constant* that is analogous to a sampling interval.

The particular generating function considered here is the *cubic B-spline*, a piecewise cubic polynomial that has continuous first- and second-order derivatives (Fig. 1, thick line):

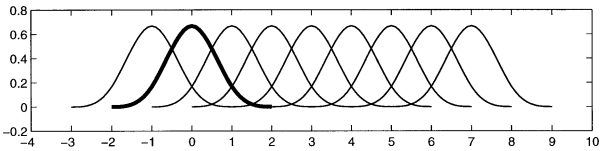

FIG. 1. The cubic B-spline generating function (thick line) and a composite of the spline basis functions (all lines) that expand over the spatial domain $0 \le x \le 6$ for the resolution $\Delta x = 1$. Note that $M = 6$ and that there are $M + 3$ basis functions centered at $x = -1, 0, \ldots, M + 1$.

$$\phi(x) = \begin{cases} \dfrac{1}{6}(x+2)^3, & -2 \le x \le -1, \\ \dfrac{2}{3} - x^2\left(1 + \dfrac{x}{2}\right), & -1 \le x \le 0, \\ \dfrac{2}{3} - x^2\left(1 - \dfrac{x}{2}\right), & 0 \le x \le 1, \\ -\dfrac{1}{6}(x-2)^3, & 1 \le x \le 2, \\ 0, & \text{otherwise.} \end{cases} \tag{6}$$

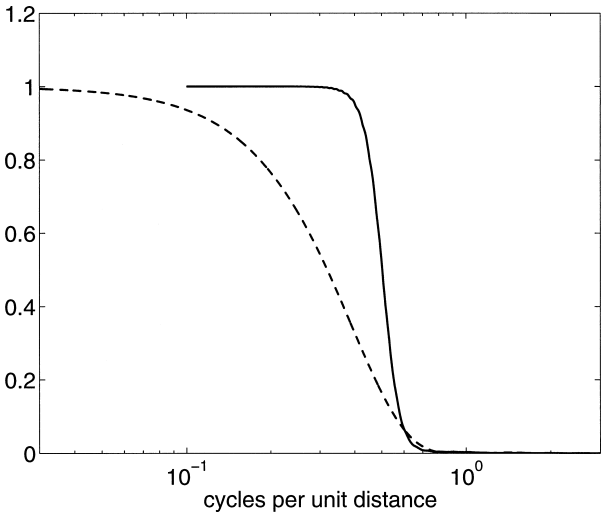

FIG. 2. The magnitude spectrum of the transfer function for the spline representation (4) when the basis function ϕ is the cubic B-spline (solid line), and the Fourier transform of the cubic B-spline generating function (dotted line). The unit distance is the spline scale Δx.

Prenter (1975), among others, discusses alternative spline functions. The B-spline function is a nonnegative weighting function [$\phi(x) \ge 0$; $\int_{-\infty}^{\infty} \phi(x)\, dx = 1$] suitable as an interpolator in general and applied to many geophysical analysis problems (e.g., Inoue 1986; Bauer et al., 1998; Chin et al. 1998). It is also a strictly local function {$\phi(x) = 0$ for $x \notin [-2, 2]$} desirable for numerical efficiency. The cubic B-spline expands each spatial coordinate $0 \le x_i \le X_i$ using $M_i + 3$ basis functions, where $M_i \Delta x_i = X_i$, while the spatial index has the range $-1 \le m_i \le M_i + 1$. See Fig. 1 for an illustration. The domain $\mathcal{M}$ of the spline coefficients is the cross-product of the ranges for all m_i. The total number of the spline coefficients $u_{j\mathbf{m}}$ used to parameterize the unknown $u_j(\mathbf{x})$ is hence $\Pi_{i=1}^{I} (M_i + 3)$.

The scale constant Δx is a critical parameter that determines the smoothness of the spline-represented fields. Smoothness can be quantified in the wavenumber domain. The Fourier transform of the cubic B-spline is $[\sin(\omega/2)/(\omega/2)]^4$, where ω is the wavenumber (e.g., Mallat 1998, p. 155). Due to the smoothness of $\phi(x)$, the spline representation (4) implicitly performs a low-pass filtering operation. The power spectral density of $\phi(x)$ indeed displays an e-folding drop-off at around 0.25 cycles per Δx, or a wavelength of $4\Delta x$ (Fig. 2, dashed line). For the full spline representation (4), this resolution improves slightly due to overlaps among the basis functions located uniformly at an interval of Δx (Fig. 1). The mean energy ratio between the spline-represented and original versions of sinusoidal waveforms (Fig. 2, solid line) indicates that the e-folding drop-off is around a wavelength of $2\Delta x$. This implies that, to represent a feature whose smallest wavelength is $L \equiv 2\pi/\omega$, the spline scale Δx needs to be smaller than $L/2$. Knowing such a physically based upper limit for Δx is useful, as it is computationally advantageous to choose the largest possible value to minimize the number of unknown spline coefficients. Figure 3 shows a 2000 km by 2000 km velocity field (from a numerical simulation; see section 3) and its representations by cubic B-spline of various scales. The majority of the spectral energy of the original velocity field (Fig. 3a) is contained within wavelengths of 200 km and longer. The largest scale constant Δx appropriate for this field would thus be 100 km. The spline representation with $\Delta x = 100$ km (Fig. 3c) does indicate an accurate representation, with accuracy comparable to a finer-scale representation ($\Delta x = 50$ km; Fig. 3b). Both of these approximation fields have normalized approximation errors of only about 2%. For splines with $\Delta x > 100$ km, the errors increase sharply (e.g., 58% for $\Delta x = 400$ km), and misrepresentation of the field becomes visibly apparent (Figs. 3d–f).

c. *Variational-spline solution*

Solution of the variational-spline problem is to evaluate the spline coefficients $\mathbf{u}_{j\mathbf{m}}$ given the model parameters $\mathbf{a}_{j\mathbf{n}}$ and $\mathbf{b}$, the observation parameters c_{jk}, and the data ($\mathbf{x}_k^d$, d_k). This evaluation is realized by substituting (4) into (3) and then finding $\mathbf{u}_{j\mathbf{m}}$ that minimizes (3). This procedure can be accomplished by solving for the resulting, discrete version of the Euler–Lagrange equation, which is a linear system of equations written as (cf. section 7.1 of Prenter 1975)

$$\sum_{j=1}^{J} \sum_{\mathbf{m} \in \mathcal{M}} E_{j'\mathbf{m}'j\mathbf{m}} u_{j\mathbf{m}} = F_{j'\mathbf{m}'}, \tag{7}$$

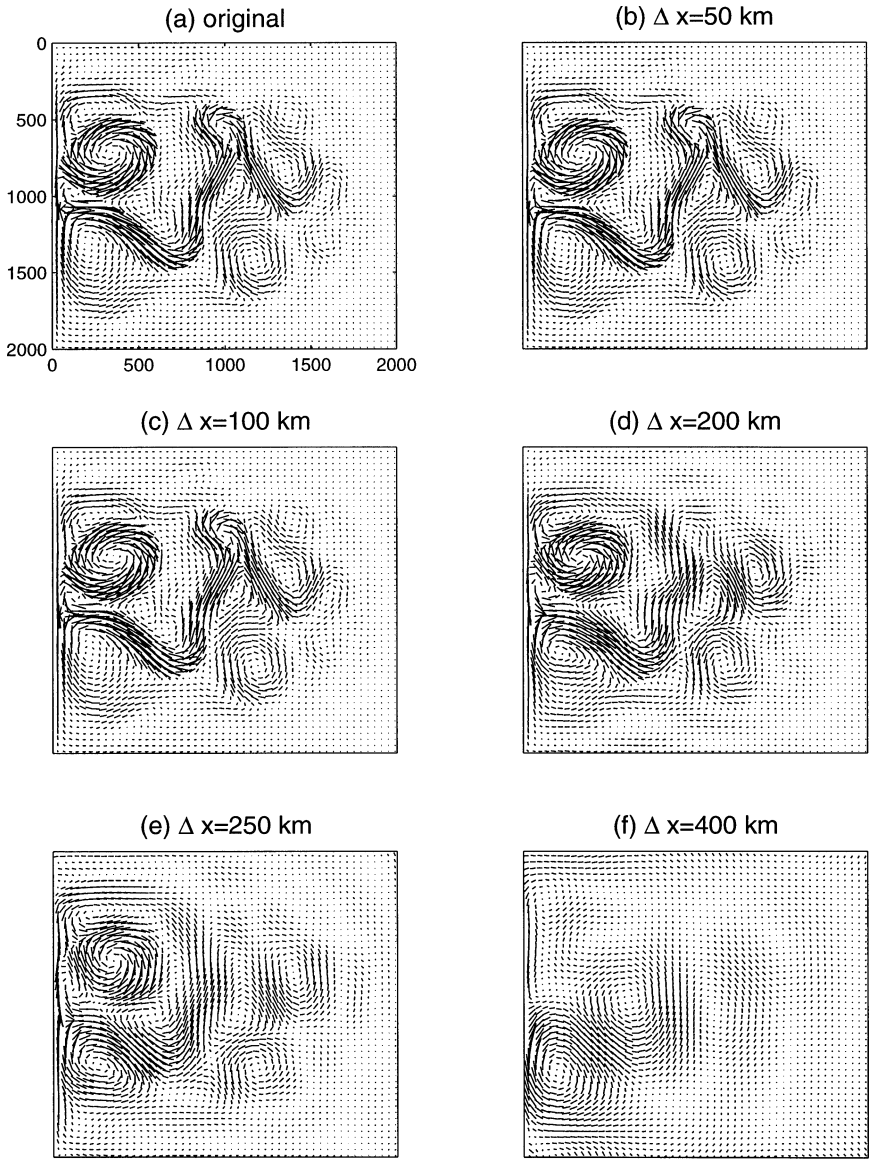

FIG. 3. (a) A 2000 km by 2000 km velocity field over a 20-km grid and its cubic B-spline approximations using spline basis of various scales Δx = (b) 50, (c) 100, (d) 200, (e) 250, and (f) 400 km.

for $j' = 1, 2, \ldots, J$ and $m_i' = -1, 0, \ldots, M_i + 1$, where $i = 1, \ldots, I$. The coefficients of the equations are given as

$$E_{j'\mathbf{m}'j\mathbf{m}} = \sum_{\mathbf{n}'\in\mathcal{N}}\sum_{\mathbf{n}\in\mathcal{N}} [\mathbf{a}_{j',\mathbf{n}'}^{\mathrm{T}}\mathbf{Q}^{-1}\mathbf{a}_{j\mathbf{n}}]S_{\mathbf{m}'\mathbf{m}}^{(\mathbf{n}',\mathbf{n})} + \sum_{k=1}^{K} c_{kj'}c_{kj}R_k^{-1}\phi_{m'}(\mathbf{x}_k^d)\phi_{\mathbf{m}}(\mathbf{x}_k^d) \quad \text{and} \tag{8}$$

$$F_{j'\mathbf{m}'} = \sum_{\mathbf{n}'\in\mathcal{N}} [\mathbf{a}_{j',\mathbf{n}'}^{\mathrm{T}}\mathbf{Q}^{-1}\mathbf{b}]S_{\mathbf{m}}^{(\mathbf{n}')} + \sum_{k=1}^{K} c_{kj'}\phi_{\mathbf{m}'}(\mathbf{x}_k^d)R_k^{-1}d_k, \tag{9}$$

where $S_{\mathbf{m}'\mathbf{m}}^{(\mathbf{n}',\mathbf{n})}$ and $S_{\mathbf{m}}^{(\mathbf{n})}$ are constants dependent only on the spline-generating function and can be precomputed offline as described below. The terms in square brackets are scalars, and many of them are zero, making the summation manageable. The precomputable constants are given as

$$S_{\mathbf{m}'\mathbf{m}}^{(\mathbf{n}',\mathbf{n})} \equiv \int_{\mathcal{D}} \nabla^{\mathbf{n}'}\phi_{\mathbf{m}'}\nabla^{\mathbf{n}}\phi_{\mathbf{m}}\, d\mathbf{x} = \prod_{i=1}^{I} S_{m_i'm_i}^{(n_i',n_i)} \tag{10}$$

$$S_{\mathbf{m}}^{(\mathbf{n})} \equiv \int_{\mathcal{D}} \nabla^{\mathbf{n}}\phi_{\mathbf{m}}\, d\mathbf{x} = \prod_{i=1}^{I} S_{m_i}^{(n_i)}, \tag{11}$$

where the terms $S_{m'm}^{(n',n)}$ and $S_{m'}^{(n')}$ denote the definite integrals

$$S^{(n',n)}_{m',m} \equiv \int_0^X \frac{\partial^{n'}}{\partial x^{n'}}\phi_{m'}(x)\frac{\partial^{n}}{\partial x^{n}}\phi_{m}(x)\,dx \quad \text{and}$$

$$S^{(n)}_{m} \equiv \int_0^X \frac{\partial n}{\partial x^{n}}\phi_{m}(x)\,dx,$$

which can be precomputed (offline) as a rational number scaled by Δx, as

$$S^{(n',n)}_{m',m} = (\Delta x)^{1-n'-n}N^{(n',n)}_{m',m}/D^{(n',n)} \quad \text{and}$$

$$S^{(n)}_{m} = (\Delta x)^{1-n}N^{(n)}_{m}/D^{(n)}.$$

Compared to the univariate spline (Inoue 1986), a multivariate spline must incorporate a significantly larger number of these integration constants. The values of the integers N and D for the cubic B-spline are tabulated in Tables 1–3. Since the basis function $\phi(x)$ is strictly local, a vast majority of these integral constants are zero. In particular, when (7) for the cubic B-spline is written as a single matrix–vector equation, the matrix operator would have a sparse, nested block septadiagonal structure. The matrix operator is also symmetric ($E_{j\mathbf{m}j'\mathbf{m}'} = E_{j'\mathbf{m}'j\mathbf{m}}$) and positive definite.

d. Computational considerations

The numerical tasks necessary for the variational spline analysis given the model (1) and data (2) would essentially amount to solving the linear system of Eq. (7). Once the unknown coefficients $u_{j\mathbf{m}}$ are evaluated, the physical variables can be analyzed at the desired locations $\mathbf{x}$ using (4). Solution of the linear equations (7) is also responsible for nearly the entire computational cost of the variational spline analysis. The number ℓ of the unknowns can be large, as $\ell = J\prod_{i=1}^{I}(M_i + 3)$; however, (7) is a sparse, symmetric, and positive definite system for which efficient solvers are readily available. We have used the conjugate gradient method, a standard iterative linear system solver, whose computational cost per iteration is contributed essentially by a single matrix–vector multiplication. In particular, due to the block septadiagonal structure of (7), each iteration can be performed with at most $(7^I + 10)\ell$ floating point operations, and the solution converges geometrically as the approximation error is reduced at least by a factor of $(\sqrt{\kappa} - 1)/(\sqrt{\kappa} + 1)$ after each iteration, where κ is the condition number for the linear operator (Golub and van Loan 1989). Convergence of the conjugate gradient solver is thus especially fast if the condition number κ is close to 1, that is, if all eigenvalues of the linear operator have comparable magnitudes. In practice, ''nondimensionalization'' of the analysis model (1) and some crude balancing of dynamic ranges among the variables, that is, normalization of each type of variable u_j by its perceived or empirical variability, can improve the numerical conditioning enough to greatly enhance the convergence speed. In the case studies described next ($I = 2$, $J = 3$, $\ell = 30\,000$), the

TABLE 1. Values of $N^{(n',n)}_{m',m}$ for the cubic B-spline function up to the second-order derivatives for $0 \le x \le M\Delta x$. Note that $m,m' \in [-1, M]$ and $N^{(n,n')}_{m,m'} = N^{(n',n)}_{m',m}$. Each row of the tables corresponds to a value of m', while each column is a value of $m' - m$. Entries not found in the table are all null. Entries marked by * do not exist.

$N^{(0,0)}$

m' \ $m-m'$	−3	−2	−1	0	1	2	3
−1	*	*	*	20	129	60	1
0	*	*	129	1208	1062	120	1
1	*	60	1062	2396	1191	120	1
2 ~ M −2	1	120	1191	2416	1191	120	1
M − 1	1	120	1191	2396	1062	60	*
M	1	120	1062	1208	129	*	*
M + 1	1	60	129	20	*	*	*

$N^{(1,1)}$

m' \ $m-m'$	−3	−2	−1	0	1	2	3
−1	*	*	*	6	7	−12	−1
0	*	*	7	40	−22	−24	−1
1	*	−12	−22	74	−15	−24	−1
2 ~ M −2	−1	−24	−15	80	−15	−24	−1
M − 1	−1	−24	−15	74	−22	−12	*
M	−1	−24	−22	40	7	*	*
M + 1	−1	−12	7	6	*	*	*

$N^{(2,2)}$

m' \ $m-m'$	−3	−2	−1	0	1	2	3
−1	*	*	*	2	−3	0	1
0	*	*	−3	8	−6	0	1
1	*	0	−6	14	−9	0	1
2 ~ M −2	1	0	−9	16	−9	0	1
M − 1	1	0	−9	14	−6	0	*
M	1	0	−6	8	−3	*	*
M + 1	1	0	−3	2	*	*	*

$N^{(0,1)}$

m' \ $m-m'$	−3	−2	−1	0	1	2	3
−1	*	*	*	−10	−9	18	1
0	*	*	−71	−160	174	56	1
1	*	−38	−254	−10	245	56	1
2 ~ M −2	−1	−56	−245	0	245	56	1
M − 1	−1	−56	−245	10	254	38	*
M	−1	−56	−174	160	71	*	*
M + 1	−1	−18	9	10	*	*	*

$N^{(0,2)}$

m' \ $m-m'$	−3	−2	−1	0	1	2	3
−1	*	*	*	4	−7	2	1
0	*	*	33	−40	−18	24	1
1	*	22	22	−84	15	24	1
2 ~ M −2	1	24	15	−80	15	24	1
M − 1	1	24	15	−84	22	22	*
M	1	24	−18	−40	33	*	*
M + 1	1	2	−7	4	*	*	*

$N^{(1,2)}$

m' \ $m-m'$	−3	−2	−1	0	1	2	3
−1	*	*	*	−3	5	−1	−1
0	*	*	−5	0	14	−8	−1
1	*	7	−14	−3	19	−8	−1
2 ~ M −2	1	8	−19	0	19	−8	−1
M − 1	1	8	−19	3	14	−7	*
M	1	8	−14	0	5	*	*
M + 1	1	1	−5	3	*	*	*

TABLE 2. Values of $N_m^{(n)}$ for the cubic B-spline function up to the second-order derivatives for $0 \le x \le M\,\Delta x$.

m	$N^{(0)}$	$N^{(1)}$	$N^{(2)}$
-1	1	-1	1
0	12	-4	0
1	23	-1	-1
$2 \sim M-2$	24	0	0
$M-1$	23	1	-1
M	12	4	0
$M+1$	1	1	1

results displayed have been obtained within 50 iterations. Moreover, because the operator in (7) is *local* (in the sense of distance in the physical domain), the computation is highly scalable for parallel implementation.

3. Numerical experiments

To demonstrate the variational-spline analysis, we have created synthetic sea surface altimetry and drifting-buoy datasets using a numerical simulation of idealized ocean circulation, which has a horizontal domain size of 2000 km $\times$ 2000 km, Rossby radius of roughly 40 km, and grid size of 20 km capable of resolving mesoscale features. We wish to compute a multivariate analysis of the horizontal velocity (u, v) and surface topography h fields over the horizontal space (x, y). The prior model considered here consists of the geostrophic balance

$$fu + g'\frac{\partial}{\partial y}h = 0, \qquad fv - g'\frac{\partial}{\partial x}h = 0, \quad (12)$$

where f is the Coriolis frequency and g' is the reduced gravity constant, and the so-called thin-plate model (Bookstein 1989) applied only to the h field as

$$\frac{\partial^2}{\partial x^2}h = 0, \qquad \frac{\partial^2}{\partial y^2}h = 0, \qquad \frac{\partial^2}{\partial x \partial y}h = 0 \quad (13)$$

to promote smoothness of the material surface. We refer to this analysis model as the *geostrophy–thin-plate* (GT) analysis model. By differentiating both sides of (12), assuming that $(\partial f/\partial y)/f \approx 0$, and combining with (13), we have a constraint for the relative vorticity ζ as

$$\zeta \equiv \frac{\partial}{\partial x}v - \frac{\partial}{\partial y}u = \left(\frac{g'}{f}\right)\left(\frac{\partial^2}{\partial x^2} + \frac{\partial^2}{\partial y^2}\right)h = 0, \quad (14)$$

which indicates that the GT model is an expression for conservation of the relative vorticity.

The GT model [(12), (13)] can be written in the generic vector form of the model equation (1), with $I = 2$ and $J = 3$. Only six (out of possible $3 \times 3^2 = 27$, assuming $N_i = 2$ for each i) $\mathbf{a}_{j\mathbf{n}}$ are nonzero vectors, each with only a single nonzero component. The covariance matrix $\mathbf{Q}$ used here is an identify matrix; correlations exhibited among the variables are entirely due to the analysis model. For the observations, we used $\mathbf{R}_k = 0.1$. Only the ratio between these variance values is relevant to the outcome of the analysis. The spline scale used is $\Delta x = \Delta y = 80$ km, with a wavelength resolution of roughly 160 km.

TABLE 3. Values of $D^{(n',n)}$ and $D^{(n)}$ for the cubic B-spline function up to the second-order derivatives. Note that $D^{(n,n')} = D^{(n',n)}$.

$D^{(0,0)}$	$D^{(1,1)}$	$D^{(2,2)}$	$D^{(0,1)}$	$D^{(0,2)}$	$D^{(1,2)}$	$D^{(0)}$	$D^{(1)}$	$D^{(2)}$
5040	120	6	720	120	24	24	6	2

a. Sea surface altimetry

Figure 4a shows an h field with sampling tracks of the TOPEX/Poseidon satellite, which has a repeat cycle of 10 days. The full, 10-day sampling pattern is shown with dots, with the darker dots indicating a partial set of the sampling points over an arbitrary 5-day period.

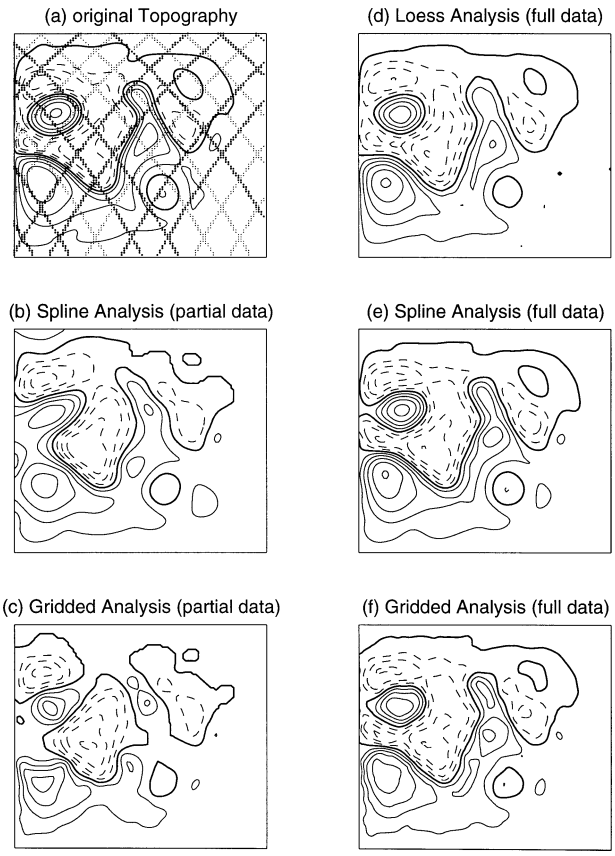

FIG. 4. (a) Sea surface topography field, with solid (dashed) contours representing positive (negative) elevations, and TOPEX/Poseidon satellite tracks over a partial 5-day period (dark dots) and a full 10-day repeat-cycle period (light and dark dots); (b) interpolation of the 5-day partially sampled data from (a) using the variational spline technique; (c) same as (b) except computed using finite differencing over a gridded space; (d) interpolation of the 10-day fully sampled data from (a) using the loess technique; (e) the same as (d) except using the variational spline technique; (f) same as (e) except computed using finite differencing over a gridded space.

For demonstration purposes, the data sampling is performed synoptically (i.e., time-dependent variability is not included in the analysis problem) in this example. The h fields sampled under these tracks are then analyzed to reconstruct the (u, v, h) fields. Figure 4b (using the 5-day samples) and Fig. 4e (using the 10-day samples) show the corresponding analyses of the h field by the multivariate variational spline. The velocity fields (not shown) tend to be geostrophically aligned with the contour lines.

The spline-based analyses (Figs. 4b,e) are compared to solutions of the same variational formulation computed without the spline basis, using the first-order center differencing for discretization instead (Figs. 4c,f, respectively). The result is clearly favorable for the spline-based solution, with respect to both the utility of the analysis and computational efficiency. For the spline-based analysis (Fig. 4b), major features of the circulation pattern are already emerging using only half (5 days' worth) of the available data, while the corresponding finite-difference solution (Fig. 4c) is corrupted by the sampling artifacts indicative of the satellite tracks (Fig. 4a, dark dots). Computationally, the number of spline coefficients required to be evaluated for the analysis is only 1/4 of the number of variables in the finite-difference approach.

The spline-based analysis (Fig. 4e) is also compared to a univariate analysis (Fig. 4d) based on the locally weighted regression (*loess*) technique, a commonly used method for satellite altimetry data (Chelton and Schlax 1994), where a cubic polynomial is fit *locally* at each grid point by least squares using a particular weighting scheme (Cleveland 1979; with the smoothness/resolution parameter set at "q/n" = 10%). While the analyses by the two techniques are comparable in accuracy for the most part, the loess technique has required sensitive adjustments of a parameter that trades off the resolution of the analysis with spatial consistency in smoothness. The variational spline technique has maintained numerical stability at least around the resolution examined. An advantage of the spline-based technique is that the analysis resolution can be specified explicitly (as the spline-scale values). The technique does require more computational resources than a strictly local technique such as loess, especially when the domain dimension I increases.

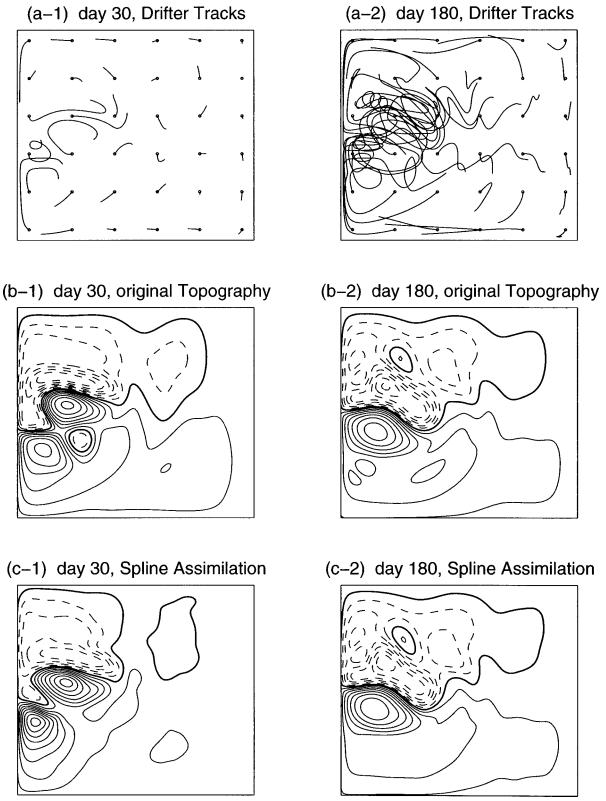

FIG. 5. (a) Model-simulated tracks of tracers ("drifters"), where the small circles represent the initial release locations; (b) the surface topography field of the same model simulation; (c) a different model run (initialized from the rest), where the velocity estimates from the tracer tracks have been interpolated by the variational spline and then assimilated into the model state each day. The left-hand (right-hand) column displays the results after 30 days (180 days) of model simulation.

b. Drifting buoy

In the altimetry example above, the velocity field could have been computed geostrophically (12) by differentiating a *univariate* analysis of the topography (h) field. On the other hand, the problem of interpolating the topography field based on sparse velocity measurements is a more critical test for a multivariate analysis method because the velocity data interact with the topography field only *implicitly* through the differential operators of the geostrophy equations. The h field can hence be evaluated up to variations about an unknown constant, such as the mean surface height. In the example considered here, the (u, v) data are derived from simulated drifter (drifting buoy) tracks.

The drifters are instruments for Lagrangian-coordinate sampling of watermass transport. A set of drifter location data is first converted into some rough ("pseudo-Lagrangian") estimates of the velocity, and is then interpolated using the multivariate B-spline. Özgökmen et al. (2003) describe the details of the experimental setup used here, including the procedures to sample the velocity field from the drifter tracks. At midlatitudes where geostrophy is valid, sparse velocity measurements can be used to reconstruct the surface topography in a remarkably efficient and effective fashion. Figure 5 shows model-simulated drifter tracks (Fig. 5a), the corresponding simulated topography fields (Fig. 5b), and multivariate-spline analysis (Fig. 5c) of the topography reconstructed from the velocity data sampled from the drifter tracks. The reconstructed velocity fields are, again, nearly geostrophic with respect to h and not shown. In the analyzed field some major topographic

features emerge by the 30th day of the simulation (cf. Fig. 5c-1 with Fig. 5b-1), while most of the identifiable features have been reconstructed by day 180 (cf. Fig. 5c-2 with Fig. 5b-2). The final (day 180) root-mean-squared difference between the analysis and original fields is approximately 10% of the average dynamic variability of *h*.

The multivariate-spline technique presents two means to spread the velocity data information horizontally. One is through the spatial extent of each basis function controlled by the spline-scale parameter, as discussed earlier. The other is the GT analysis model through the smoothness constraint (13) that can affect the velocity data only through the (weakly constraining) geostrophic balance (12). The spline analysis in this case thus accomplishes spatial interpolation through inversion of a geostrophic operator.

4. Summary and conclusions

Advances in computers can make a multivariate, multidimensional variational analysis a routine procedure. A generic recipe for a finite-element solution based on cubic B-spline has been presented. In particular, a procedure and tables of necessary constants have been given. The spline analysis can then be computed as the solution of a single, sparse linear system of equations.

An important advantage of the presented method over a more traditional technique that requires inversion of a finite-difference operator is computational efficiency. The computational grid scale (spline scale) can be chosen explicitly in terms of physical scales of features desired in the analysis. The number of unknowns can be significantly smaller than the number of grid points typically required in the finite-difference analysis, as demonstrated in the numerical examples.

Acknowledgments. This work is supported in parts by Office of Naval Research Grants N00014-95-1-0257 and N00014-99-1-0049 and by National Science Foundation Grant OCE-0136700.

REFERENCES

Bauer, S., M. S. Swenson, A. Griffa, A. J. Mariano, and K. Owens, 1998: Eddy-mean flow decomposition and eddy-diffusivity estimates in the tropical Pacific Ocean. *J. Geophys. Res.,* **103,** 30 855–30 871.

Bookstein, F. L., 1989: Principal warps: Thin-plate splines and the decomposition of deformations. *IEEE Trans. Pattern An. Mach. Intell.,* **11,** 567–585.

Chelton, D. B., and M. G. Schlax, 1994: The resolution capability of an irregularly sampled dataset: With application to Geosat altimeter data. *J. Atmos. Oceanic Technol.,* **11,** 534–550.

Chin, T. M., R. F. Milliff, and W. G. Large, 1998: Basin-scale, high-wavenumber sea surface wind fields from a multiresolution analysis of scatterometer data. *J. Atmos. Oceanic Technol.,* **15,** 741–763.

Cleveland, W. S., 1979: Robust locally weighted regression and smoothing scatterplots. *J. Amer. Stat. Assoc.,* **74,** 829–836.

Ghil, M., and P. Malanotte-Rizzoli, 1991: Data assimilation in meteorology and oceanography. *Advances in Geophysics,* Vol. 33, Academic Press, 141–266.

Golub, G. H., and C. F. van Loan, 1989: *Matrix Computations.* The Johns Hopkins University Press, 642 pp.

Inoue, H., 1986: A least-squares smooth fitting for irregularly spaced data: Finite-element approach using the cubic B-spline basis. *Geophysics,* **51,** 2051–2066.

Mallat, S. G., 1998: *A Wavelet Tour of Signal Processing.* Academic Press, 577 pp.

Özgökmen, T. M., A. Molcard, T. M. Chin, L. I. Piterbarg, and A. Griffa, 2003: Assimilation of drifter observations in primitive equation models of midlatitude ocean circulation. *J. Geophys. Res.,* **108**, 3238, doi:10.1029/2002JC001719.

Prenter, P. M., 1975: *Splines and Variational Methods.* Wiley, 323 pp.